



RESEARCH ARTICLE

Multi-optical carrier generation using a microring resonator to enhance the number of serviceable channels in radio over free space optic

I. S. Amiri, S. E. Alavi, S. Punthawanunt, P. Yupapin, P. Youplao 

First published: 27 May 2017 [Full publication history](#)

DOI: 10.1002/mop.30681 [View/save citation](#)

Cited by (CrossRef): 0 articles  [Check for updates](#)  [Citation tools](#) 



Funding Information

Funding information University of Malaya (UM), Grant Numbers: LRGS (2015)NGOD/UM/KPT, UM.C/625/1/HIR/MOHE/SCI/01, GA010-2014 (ulung), and RU007/2015



[View issue TOC](#)
Volume 59, Issue 8
August 2017
Pages 2038-2044

Abstract

A system of radio over free space optic (RoFSO) system using the multi-optical carriers has been generated by the microring resonators integrating an add/drop filter. These obtained carriers have shown sufficiently stable for propagating in free space channels while experiencing very low dispersion. Moreover, this technique is appropriated for higher capacity that can be serviced in a system of wavelength-division multiplexing (WDM) RoFSO, where there are 16 carriers created, where each carrier has 12.5 GHz free spectral range (FSR) and 220 MHz full-width at half-maximum (FWHM) and 8 orthogonal frequency division multiplex (OFDM) signals, then they separately modulated with 8 out of these 16 carriers. After the modulation, by utilizing an free space optic (FSO) antenna, all carriers have the optical multiplexing and transmission to a FSO channel. On the receiver side, the demultiplexing is performed and finally the performance of the system subsequently is analyzed by calculation of the constellation diagram and error vector magnitude (EVM).

Multi-Optical Carrier Generation Using a Microring Resonator to Enhance the Number of Serviceable Channels in RoFSO

I.S. Amiri¹, S.E. Alavi², S. Punthawanunt³, P. Youplao^{4,5*}, P. Yupapin^{4,5}

¹Photonics Research Centre, University of Malaya, 50603 Kuala Lumpur, Malaysia;

²Faculty of Electrical Engineering, Universiti Teknologi Malaysia, 81310 UTM Johor Bahru Malaysia

³Interdisciplinary Research Center, Faculty of Science and technology, Kasem Bundit University, Bangkok 10250, Thailand;

⁴Department for Management of Science and Technology Development, Ton Duc Thang University, District 7, Ho Chi Minh City, Vietnam;

⁵Faculty of Electrical & Electronics Engineering, Ton Duc Thang University, District 7, Ho Chi Minh City, Vietnam;

*Corresponding author E-mail: pichai.youplao@tdt.edu.vn

Abstract: A system of radio over free space optic (RoFSO) system using the multi-optical carriers has been generated by the microring resonators integrating an add/drop filter. These obtained carriers have shown sufficiently stable for propagating in free space channels while experiencing very low dispersion. Moreover, this technique is appropriated for higher capacity that can be serviced in a system of wavelength-division multiplexing (WDM) RoFSO, where there are sixteen carriers created, where each carrier has 12.5 GHz free spectral range (FSR) and 220 MHz full-width at half-maximum (FWHM) and eight orthogonal frequency division multiplex (OFDM) signals, then they separately modulated with eight out of these sixteen carriers. After the modulation, by utilizing an FSO antenna, all carriers have the optical multiplexing and transmission to a free space optic (FSO) channel. On the receiver side, the de-multiplexing is performed and finally, the performance of the system subsequently analyzed by calculation of the constellation diagram and error vector magnitude (EVM).

Keywords: Microring resonator; radio over free space optic (RoFSO), Optical component

1. Introduction

In last few years, broadband suppliers have received increasing demands to provide higher data rates for the purposes of supporting a variety of new services and greater numbers of users [1, 2]. The free space optical (FSO) systems are studied as a predicting candidate to satisfy the demands associated with the emerging generation of broadband consuming services. In cases of impractical connection between components, the FSO links which refer to as radio-on-free space optics (RoFSO), can be utilized to carry the signals which are in the range of radio frequencies (PFs) signals. The capability of RoFSO is comparable with the radio over fiber (RoF), but there is a difference which is the omission of the fiber medium. Benefits from using high transmission capacity together with the ease of deployment associated with wireless links are the other differences [3, 4]. RoFSO has also found applications within indoor optical broadcasting. A practical research of indoor optical wireless link is shown in details in a report [5]. In this study, a range of 1550-nm wavelength was included a uni-directional cable television (CATV) signal, and a bi-directional link, where the bi-directional link itself consisting of two 10 Gbps data links. In regards to outdoor applications, the operation of a deployed

RoFSO is extremely determined by the environment features such as dense weather conditions (rain, snow, fog, dust particles etc). These would result in a fade in the received signal and consequently reducing the link performance. The refractive-index random variations will cause significant distortions on the transmitted beam leading to the annihilation of the FSO link. To sustain the stability of signals is the major concerns in RoFSO communication systems [6]. Wavelength-division multiplexing (DWDM) RoFSO system is studied by preliminary experimental efforts in various research works [3, 5]. Figure 1 shows the DWDM RoFSO system.

A RoFSO link has a capacity for heterogeneous wireless services equivalent to that for RoF. An orthogonal frequency division multiplexing (OFDM) can be utilized to expanding broadband access [7]. OFDM can be used for RoFSO as described experimentally in References [8, 9]. The OFDM based RoFSO technology mostly have contributed in regards to the possibility of implementation of the system and have not focused on higher capacity. A higher stability and reliable signals are typically considered as the principal requirements. In this work we have generated a greater number and more stable multi-carriers, so that the consequent increase in WDM

channels can be performed in the capacity of the RoFSO system. In the research described in this paper, the microring resonators integrated with optical add/drop filter are used to produce many optical carriers for application in a RoFSO system. Moreover, the ring was controlled via manipulation of variable system parameters [10]. An analysis is presented regarding performance evaluation of the RoFSO system.

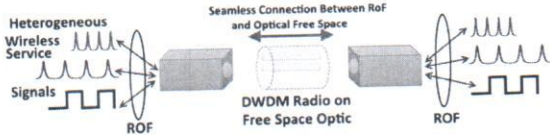


Fig. 1. RoFSO system

2. Multicarrier generation

Figure 2 shows the proposed microring resonators. Here, three microring resonators are connected with an add/drop filter. The InGaAsP/InP waveguides are used for simulating of the microring resonators. The filtering stages of the input are performed by using three microring resonators, where the frequency comb, ranges from 193.15 to 193.65 THz achieved. In order to construct the microring resonator waveguide, few materials layers are used. Each layer has its thickness and particular refractive index. The input wave will be guided through the waveguide structure. In this case, the InGaAsP/InP waveguide has the parameters as shown in Table 1.

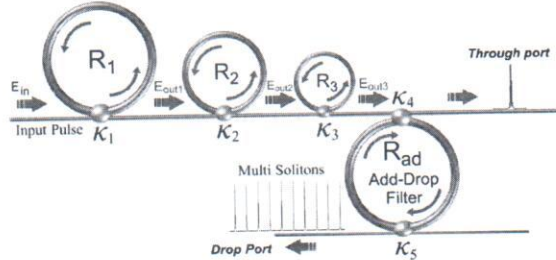


Fig. 2. System of microring resonator with R : ring's radius, κ : coupling coefficients, R_{ad} : add/drop ring's radius, E_{in} : input power, E_m : Ring resonator output E_t : throughput output, and E_d : drop port output

Table-1: Waveguide parameters

Layer number (from bottom to top)	Materials used	Thickness (μm)	Refractive index
1	InP substrate	1.5	3.18
2	InGaAsP	0.3	3.34
3	InGaAsP (etch stop layer)	0.04	3.39
4	InGaAsP	0.5	3.34
5	InP cap	0.7	3.18

The medium of the ring resonator has Kerr effect-type nonlinearity [11, 12], therefore variation of the total refractive index can be presented in Equation 1.

$$n = n_0 + n_2 I = n_0 + \frac{n_2}{A_{eff}} P \quad (1)$$

The n_0 and n_2 are linear and nonlinear refractive indices, and the optical intensity and power are shown by I and P respectively [13]. The effective mode core area of the system is shown by A_{eff} . The center frequency of the input spectrum is $1.55 \mu\text{m}$, where the peak power is 1.2 W. The electrical component of the input is given as follows [14].

$$E_m(t, z) = E_0 \exp \left[\left(\frac{iz}{2L_D} \right) - i\omega_0 t \right] \quad (2)$$

E_0 representing the amplitude and z is the propagation distance. The dispersion length is defined by L_D and ω_0 is the carrier frequency [15, 16]. The output intensity after each microring resonators (from the three integrated microring resonators), can be expressed by

$$\left| \frac{E_m(t)}{E_n(t)} \right|^2 = (1-\gamma) \left[1 - \frac{(1-(1-\gamma)x^2)\kappa}{(1-x\sqrt{1-\gamma}\sqrt{1-\kappa})^2 + 4x\sqrt{1-\gamma}\sqrt{1-\kappa}\sin^2(\frac{\phi}{2})} \right] \quad (3)$$

The following table (table number 2) show the parameters used in the Equation 3 [17].

Table-2: The used parameters

Parameters	Definition
$x = \exp(-\alpha L / 2)$	Round trip loss coefficient
κ	Coupling coefficient
L	Ring resonator length
α	Absorption coefficient
$\phi = \phi_0 + \phi_{NL}$	Total phase
$\phi_0 = k_n L n_0$	Linear phase shift
$\phi_{NL} = k_n L n_2 E_m ^2$	Nonlinear phase shift
γ	Fractional coupler intensity loss
$k_n = 2\pi / \lambda$	wave number

The outputs from each microring resonators pass through the next microring resonator, therefore the output from the third microring resonator input to the add/drop filter system. The input then will make a round-trip within the system and constructive and destructive interferences occur. The optical modes with higher power can overcome the loss within the system and be detected at the output ports. In the other words, the microring resonator consists of an optical waveguide in such a way it is looped back on itself,

therefore the resonance occurs. In order to obtain the resonance condition, the optical path length of the microring resonator should be exactly a whole number of the wavelengths [18]. The waves in the loop build up a round trip phase shift which equals to integer times 2π , therefore the constructive interferences occur thus the system is in resonance. The modes guided in the straight waveguide propagate on the core region while in the bent waveguide such as microring resonators the mode favors the outer radial boundary. In this research, the microring resonators have the large radius, where the loss due to the bending factor is negligible. The throughput and drop port output intensities of the add/drop filter system can be expressed by [19].

$$\frac{|E_i|^2}{|E_{out}|^2} = \frac{(1 - \kappa_4) - 2\sqrt{1 - \kappa_4} \cdot \sqrt{1 - \kappa_3} e^{-\frac{\alpha}{2} L_{ad}} \cos(k_s L_{ad}) + (1 - \kappa_3) e^{-\alpha L_{ad}}}{1 + (1 - \kappa_4)(1 - \kappa_3) e^{-\alpha L_{ad}} - 2\sqrt{1 - \kappa_4} \cdot \sqrt{1 - \kappa_3} e^{-\frac{\alpha}{2} L_{ad}} \cos(k_s L_{ad})} \quad (4)$$

$$\frac{|E_d|^2}{|E_{out}|^2} = \frac{\kappa_4 \kappa_3 e^{-\frac{\alpha}{2} L_{ad}}}{1 + (1 - \kappa_4)(1 - \kappa_3) e^{-\alpha L_{ad}} - 2\sqrt{1 - \kappa_4} \cdot \sqrt{1 - \kappa_3} e^{-\frac{\alpha}{2} L_{ad}} \cos(k_s L_{ad})} \quad (5)$$

where $|E_i|^2$ and $|E_d|^2$ are the intensities from the throughput and drop ports, respectively. Here, $L_{ad} = 2\pi R_{ad}$, and R_{ad} is the radius of the add/drop system. The frequency response of the throughput and drop ports is determined by the microring's diameter and also the core refractive index. In order to obtain higher mode confinement within the waveguide, the refractive index contrast between the core and cladding of the waveguide should be high. The microring resonators are so compact, therefore using multiple rings integrated to each other in an optical system can be utilized to construct higher order filters to meet various frequency response requirements [20].

3. Proposed system parameters and results

The microring resonators parameters are shown in Table 3. As shown in Figure 3, the chaotic noise can be generated while the input propagating within the system. The use of an add/drop filter system can help to obtain filtered and clear peaks. Therefore, cancellation of the noise signals can be performed by using the add/drop filter system, where specific parameters are used. For the applications of optical communications and telecommunications, therefore required signals can be retrieved from the noisy signals for specific users. Although many studies have shown many advantages of using the chaotic signals [21-23], in this research we have filtered the results to obtain signals with specific FSR and FWHM which are more detectable and free of errors. Here, signals which ranged from 193.15 to 193.65 THz, where the throughput output shows localized ultra-short signals with the full width at half-maximum (FWHM) of 25 MHz shown in Figure 3(f). Signals with FWHM of 220 MHz and free spectral range (FSR) of 12.5 GHz were generated in the drop port as shown in Figure

3(h). Signals ranges from 193.15 to 193.65 THz and shown in Figure 3(g), were generated as a consequence of the Gaussian spectrum input into the system. As shown in the results (Figure 4), the range 193.32 to 193.52 THz frequencies which include 16 multi-carriers with particular FSR of 12.5 GHz having approximately equals powers (threshold of 1.1 mW) were used. For many applications in telecommunications, spread spectrum telecommunication brought an important place in today's communication technologies. The ratio FSR/FWHM with the finesse (F) was approximately 56.81, and the Q-factor is $\sim 8.8 \times 10^5$.

Table-3: parameters of the microring resonators system

R_{ad}	R_1	R_2	R_3	κ_1	κ_2	κ_3
1.14mm	120 μ m	90 μ m	50 μ m	0.35	0.5	0.5
κ_4	κ_5	n_0	n_2 ($m^2 W^{-1}$)	A_{eff} (μm^2)	α (dBmm $^{-1}$)	γ
0.05	0.05	3.34	2.2×10^{-17}	4	0.5	0.1

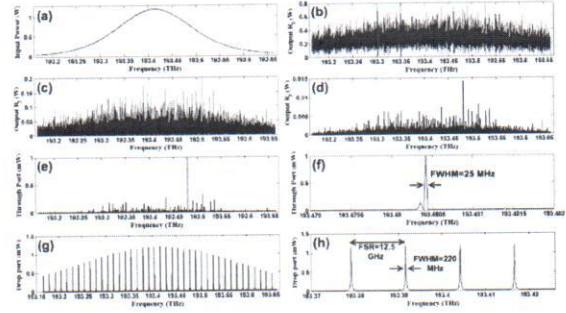


Fig. 3. (a) input Gaussian spectrum, (b) first ring's output, (c) second ring's output, (d) third ring's output, (e) results from the throughput port, (f) magnification of (e), (g) drop port results, (h) magnification of (g)

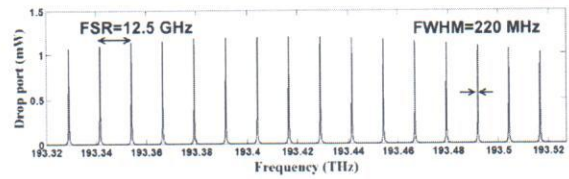


Fig. 4. Multi-output from the drop port, with FSR as 12.5 GHz and FWHM as 220 MHz

4. RoFSO system setup

Figure 5 shows the system setup for the RoFSO. A Gamma-Gamma turbulence line of sight (LOS) outdoor FSO wireless link with 1.2 km length is considered. The channel probability density function (pdf) is calculated as: [24]

$$f_{h_s}(h_s) = \frac{2\alpha\beta}{\Gamma(\alpha)\Gamma(\beta)} (h_s)^{(\alpha-\beta)/2} K_{\alpha-\beta} (2\sqrt{\alpha\beta} h_s) \quad (6)$$

The Gamma-Gamma pdf is a suitable channel model for a variety of turbulence situations [25]. Here, $K_{\alpha-\beta}(\cdot)$ is a modified Bessel function of the second kind. The $1/\beta$ and $1/\alpha$ are the variances of the small and large scale eddies, respectively. A 5 GHz OFDM signal with QPSK mapping for wireless transmission was generated on side A. Real OFDM signal generation is feasible by imposing Hermitian symmetry to the OFDM signal and a DC bias was added to the OFDM signal to make it positive. In the side A, 16 carriers generated from the ring system were separated using the de-multiplexer. By using the corresponding OFDM signals, the eight carriers ($f_1, f_3, f_5, f_7, f_9, f_{11}, f_{13}, f_{15}$) were intensity modulated as illustrated in Figure 6. The modulated and unmodulated carriers were multiplexed, then using the single mode fibers (SMF), they transmitted to the RoFSO antenna. In order to align optical wireless signal into SMF, the collimators having the parameters indicated in Table 4 were utilized for RoFSO antennas. The RoFSO antennas encompassed both amplifiers as boost and post. In the RoFSO antennas, an optical circulator is used to separate the signals from transmission and receiver parts. The RoFSO channel parameters are presented in Table 4.

Table-4: Specification of the RoFSO antenna

Parameter	Specification
Operating wavelength	1550nm
Transmit power	100 mW(20 dBm)
Antenna aperture	80mm
Coupling losses	5 dB
Beam divergence	$\pm 47.3 \mu\text{rad}$

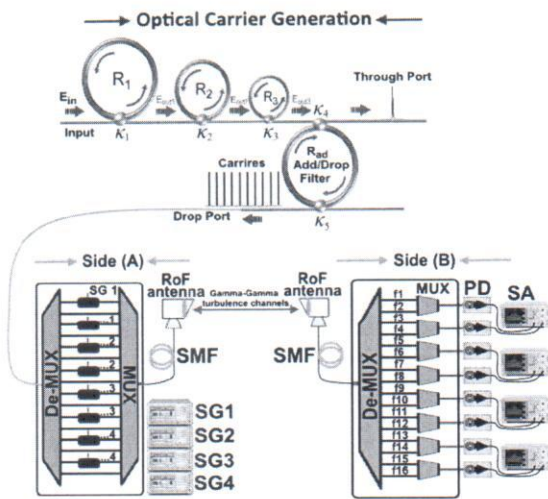


Fig. 5. A proposed system setup

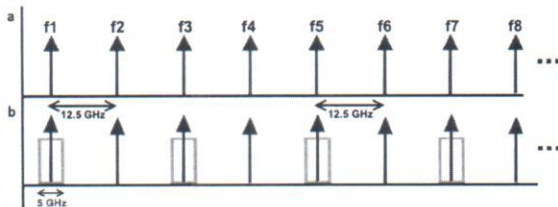


Fig. 6. (a) Carriers (b) OFDM signal (modulated)

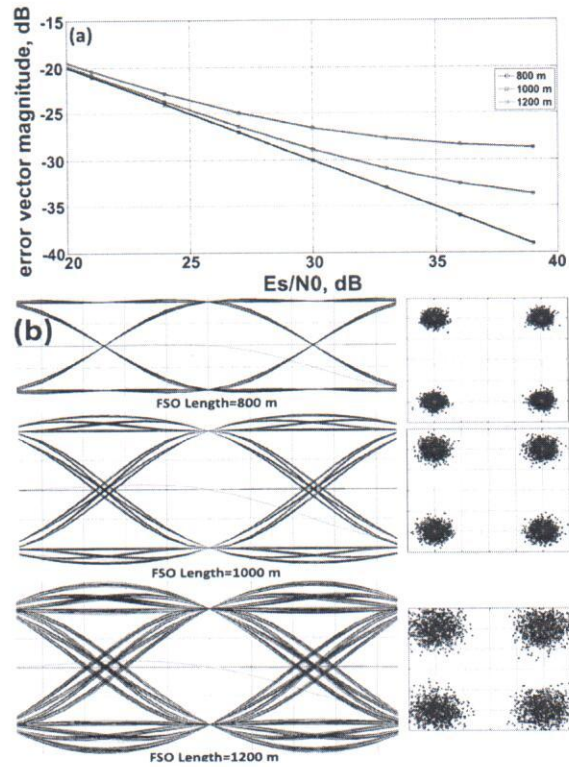


Fig. 7. (a) EVM (for 800, 1000 and 1200 meters FSO lengths), (b) related eye and constellation diagrams. As can be observed in Figure 7, acceptable EVM has been achieved for the signal to noise ratio, and the corresponding eye diagrams are indicative of successful OFDM reception.

The signal analyzers are shown on side B. The two carriers which are modulated and un-modulated having a 12.5 GHz frequency spacing (for instance f_1 and f_2) were multiplexed and converted to a 12.5 GHz RF signal using a photodiode (PD). This can be done by beating two optical beams, where one center frequency can be generated. Thus, a total of eight RoFSO channels were developed via this method. For a downlink stream, the system error vector magnitude (EVM) performance was analyzed, considering one signal of an OFDM-based RoFSO system. Here, the FSO length of three different distances as 800, 1000 and 1200 meters was supported by the test, where the EVM variation result against signal to noise ratio is shown in Figure 7.

5. Conclusion

For the proposed RoFSO system the series of microring resonators incorporating with add/drop filter was used to generate stable optical carriers. The generated carriers had great stability and low dispersion and thus were highly suitable for transmission across a free space channel. The method of generation furthermore increased the channel's number which is an advantage to support a WDM RoFSO system. The generated sixteen carriers which have FSR and FWHM of 12.5 GHz and 220 MHz, underwent a de-multiplexing and separated, where eight of them were modulated with the OFDM signals and the other eight unmodulated. These carriers (both modulated and un-modulated) were then multiplexed to be transmitted via the FSO channel by utilizing suitable antennas. Measurements of the received RF signal performance across several FSO lengths were evaluated, and the EVM results deemed acceptable. The proposed method, which was successfully demonstrated as described in this paper, therefore can be used to service more channels in RoFSO systems and so enhance broadband capacity.

Acknowledgments

I.S. Amiri would like to acknowledge the grant number LRG5 (2015)NGOD/UM/KPT, UM.C/625/1/HIR/MOHE/SCI/01, GA010-2014 (ulung) and RU007/2015 from the university of Malaya (UM).

References

- [1] N. Madamopoulos, V. Kaman, S. Yuan, O. Jerphagnon, R. J. Helkey, and J. E. Bowers, "Applications of large-scale optical 3D-MEMS switches in fiber-based broadband-access networks," *Photonic network communications*, vol. 19, pp. 62-73, 2010.
- [2] E. Wong, "Next-Generation Broadband Access Networks and Technologies," *Journal of lightwave technology*, vol. 30, pp. 597-608, 2012.
- [3] K. Kazaura, K. Wakamori, M. Matsumoto, T. Higashino, K. Tsukamoto, and S. Komaki, "RoFSO: a universal platform for convergence of fiber and free-space optical communication networks," *Communications Magazine, IEEE*, vol. 48, pp. 130-137, 2010.
- [4] M. Soltanian, H. Ahmad, C. Pua, and S. Harun, "Tunable microwave output over a wide RF region generated by an optical dual-wavelength fiber laser," *Laser Physics*, vol. 24, p. 105116, 2014.
- [5] M. Matsumoto, K. Kazaura, K. Wakamori, T. Higashino, K. Tsukamoto, and S. Komaki, "Experimental Investigation on a Radio-on-free-space Optical System Suitable for Provision of Ubiquitous Wireless Services," *PIERS Online*, vol. 6, pp. 400-405, 2010.
- [6] C. B. Naila, K. Wakamori, M. Matsumoto, A. Bekkali, and K. Tsukamoto, "Transmission analysis of digital TV signals over a radio-on-FSO channel," *Communications Magazine, IEEE*, vol. 50, pp. 137-144, 2012.
- [7] I. S. Amiri, S. E. Alavi, S. M. Idrus, A. S. M. Supaat, J. Ali, and P. P. Yupapin, "W-Band OFDM transmission for radio-over-fiber link using solitonic millimeter wave generated by MRR," *IEEE Journal of Quantum Electronics*, vol. 50, pp. 622-628, 2014.
- [8] A. Mostafa and S. Hranilovic, "In-field demonstration of OFDM-over-FSO," *Photonics Technology Letters, IEEE*, vol. 24, pp. 709-711, 2012.
- [9] A. Bekkali, C. Ben Naila, K. Kazaura, K. Wakamori, and M. Matsumoto, "Transmission analysis of OFDM-based wireless services over turbulent radio-on-FSO links modeled by Gamma-Gamma distribution," *Photonics Journal, IEEE*, vol. 2, pp. 510-520, 2010.
- [10] A. Syed, G. Chaitanya, and M. Sayeh, "All optical digital logic gates library," *Journal of Optics*, pp. 1-6, 2012.
- [11] C. Teeka, S. Songmuang, R. Jomtarak, P. Yupapin, M. Jalil, I. Amiri, et al., "ASK-to-PSK Generation based on Nonlinear Microring Resonators Coupled to One MZI Arm," in *ENABLING SCIENCE AND NANOTECHNOLOGY: 2010 International Conference On Enabling Science And Nanotechnology Escinano2010*, 2011, pp. 221-223.
- [12] I. Amiri, P. Naraei, and J. Ali, "Review and theory of optical soliton generation used to improve the security and high capacity of MRR and NRR passive systems," *Journal of Computational and Theoretical Nanoscience*, vol. 11, pp. 1875-1886, 2014.
- [13] I. Amiri, M. Soltanian, S. Alavi, and H. Ahmad, "Multi wavelength mode-lock soliton generation using fiber laser loop coupled to an add-drop ring resonator," *Optical and Quantum Electronics*, vol. 47, pp. 2455-2464, 2015.
- [14] I. Amiri and J. Ali, "Optical quantum generation and transmission of 57-61 GHz frequency band using an optical fiber optics," *Journal of Computational and Theoretical Nanoscience*, vol. 11, pp. 2130-2135, 2014.
- [15] I. Amiri, S. Alavi, M. Soltanian, N. Fisal, A. Supa'at, and H. Ahmad, "Increment of access points in integrated system of wavelength division multiplexed passive optical network radio over fiber," *Scientific reports*, vol. 5, 2015.
- [16] I. Amiri, S. Alavi, N. Fisal, A. Supa'at, and H. Ahmad, "All-Optical Generation of Two IEEE802.11n Signals for 2x2 MIMO-RoF via MRR System," *IEEE Photonics Journal*, vol. 6, pp. 1-11, 2014.
- [17] I. Amiri, S. Alavi, and J. Ali, "High-capacity soliton transmission for indoor and outdoor communications using integrated ring resonators," *International Journal of Communication Systems*, vol. 28, pp. 147-160, 2015.
- [18] W. Bogaerts, P. De Heyn, T. Van Vaerenbergh, K. De Vos, S. Kumar Selvaraja, T. Claes, et al., "Silicon microring resonators," *Laser & Photonics Reviews*, vol. 6, pp. 47-73, 2012.
- [19] S. Alavi, I. Amiri, H. Ahmad, A. Supa'at, and N. Fisal, "Generation and transmission of 3x3 w-band multi-input multi-output orthogonal frequency division multiplexing-radio-over-fiber signals using micro-ring resonators," *Applied optics*, vol. 53, pp. 8049-8054, 2014.
- [20] B. E. Little, S. T. Chu, H. A. Haus, J. Foresi, and J.-P. Laine, "Microring resonator channel dropping

- filters," *Journal of lightwave technology*, vol. 15, pp. 998-1005, 1997.
- [21] A. Argyris, D. Syvridis, L. Larger, V. Annovazzi-Lodi, P. Colet, I. Fischer, *et al.*, "Chaos-based communications at high bit rates using commercial fibre-optic links," *Nature*, vol. 438, pp. 343-346, 2005.
- [22] T. Hou, L. Yi, X. Yang, J. Ke, Y. Hu, Q. Yang, *et al.*, "Maximizing the security of chaotic optical communications," *Optics Express*, vol. 24, pp. 23439-23449, 2016.
- [23] S. Nazhan, Z. Ghassemlooy, K. Busawon, A. Gholami, and N. A. Cholan, "Chaotic signal dynamics of VCSEL for secure optical communication," in *Communication Systems, Networks and Digital Signal Processing (CSNDSP), 2016 10th International Symposium on*, 2016, pp. 1-6.
- [24] A. Farid and S. Hranilovic, "Outage capacity optimization for free-space optical links with pointing errors," *Lightwave Technology, Journal of*, vol. 25, pp. 1702-1710, 2007.
- [25] M. Al-Habash, L. C. Andrews, and R. L. Phillips, "Mathematical model for the irradiance probability density function of a laser beam propagating through turbulent media," *Optical Engineering*, vol. 40, pp. 1554-1562, 2001.